Angiopoietin-2, a Natural Antagonist for Tie2 That Disrupts in vivo Angiogenesis

Peter C. Maisonpierre,* Chitra Suri,* Pamela F. Jones,*† Sona Bartunkova,* Stanley J. Wiegand, Czeslaw Radziejewski, Debra Compton, Joyce McClain, Thomas H. Aldrich, Nick Papadopoulos, Thomas J. Daly, Samuel Davis,* Thomas N. Sato,* George D. Yancopoulos*‡

Angiogenesis is thought to depend on a precise balance of positive and negative regulation. Angiopoietin-1 (Ang1) is an angiogenic factor that signals through the endothelial cell–specific Tie2 receptor tyrosine kinase. Like vascular endothelial growth factor, Ang1 is essential for normal vascular development in the mouse. An Ang1 relative, termed angiopoietin-2 (Ang2), was identified by homology screening and shown to be a naturally occurring antagonist for Ang1 and Tie2. Transgenic overexpression of Ang2 disrupts blood vessel formation in the mouse embryo. In adult mice and humans, Ang2 is expressed only at sites of vascular remodeling. Natural antagonists for vertebrate receptor tyrosine kinases are atypical; thus, the discovery of a negative regulator acting on Tie2 emphasizes the need for exquisite regulation of this angiogenic receptor system.

During embryonic development, a primitive vascular network forms by processes that involve the regulated proliferation, differentiation, migration, and association of endothelial cells (*1*). Subsequent angiogenic processes remodel this primary network to form a mature cardiovascular system. The mature vascular network of the adult is relatively stable and undergoes angiogenic remodeling only in certain situations. Angiogenesis in the adult is normally required for tissue repair and for the reshaping of female reproductive tissues that occurs during the menstrual cycle, but it can also be subverted by tumors to allow for their continued growth and metastasis (*2*).

Angiogenesis is thought to depend on a balance between endogenous positive and negative regulatory molecules (*3*). Positive regulators are the best characterized, particularly the family of factors related to vascular endothelial growth factor/vascular permeability factor (VEGF). Among proangiogenic factors, the VEGF-related factors are distinguished by their specificity for endothelial cells. The receptors for these factors are expressed primarily on cells of the endothelial lineage, although these receptors are also expressed by early precursors of the closely linked hemopoietic lineage (*4*). The critical role of VEGF-related factors during normal vascular development has been verified by examination of mice with inactivating mutations in the genes for these factors or their receptors, which can exhibit defects in the earliest stages of endothelial cell generation (*5*). Negative angiogenic regulators such as proliferin-related protein (*6*), angiostatin (*7*), and endostatin (*8*) have also been described, but their receptors, mechanisms of action, and physiological roles have not yet been defined.

Using a strategy for isolating secreted ligands of orphan receptors, we identified a new angiogenic factor, angiopoietin-1 (Ang1) (*9*). Ang1 signals through a tyrosine kinase receptor (Tie2/Tek) that is expressed only on endothelial cells and early hemopoietic cells (*10, 11*). The absence of Ang1 or its receptor causes severe vascular abnormalities in the developing mouse embryo (*12, 13*). Here, we describe a factor closely related to Ang1, termed angiopoietin-2 (Ang2), that is a naturally occurring antagonist for Ang1 and its Tie2 receptor.

Cloning of angiopoietin-2. Complementary DNAs encoding the mouse and human versions of Ang2 were isolated by low-stringency screening of human and mouse cDNA libraries, with the use of mouse Ang1 cDNA as a probe (*14*). The inferred Ang2 protein is 496 amino acids in length and has a secretion signal peptide (Fig. 1). Human and mouse Ang2 are 85%

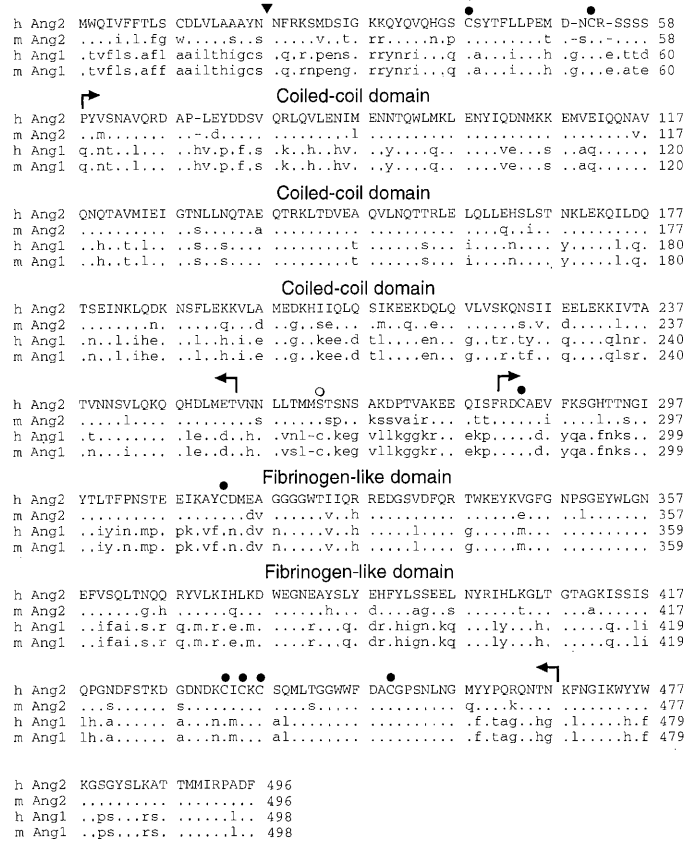

Fig. 1. Amino acid sequence comparison of mouse and human Ang1 and Ang2. Symbols: arrowhead, cleavage site for hydrophobic leader sequences; arrows, limits of the coiled-coil and fibrinogen-like domains; solid circles, conserved cysteines; open circle, a cysteine present only in Ang1; dots, amino acids identical to those in human Ang2; and dashes, a gap inserted to optimize alignment. The human and mouse Ang2 cDNA sequences have been deposited in GenBank (accession numbers AF004327 and AF004326, respectively). Abbreviations for amino acids are as follows: A, Ala; C, Cys; D, Asp; E, Glu; F, Phe; G, Gly; H, His; I, Ile; K, Lys; L, Leu; M, Met; N, Asn; P, Pro; Q, Gln; R, Arg; S, Ser; T, Thr; V, Val; W, Trp; and Y, Tyr.

P. C. Maisonpierre, C. Suri, P. F. Jones, S. J. Wiegand, C. Radziejewski, D. Compton, J. McClain, T. H. Aldrich, N. Papadopoulos, T. J. Daly, S. Davis, and G. D. Yancopoulos are at Regeneron Pharmaceuticals Inc., 777 Old Saw Mill River Road, Tarrytown, NY 10591, USA. S. Bartunkova and T. N. Sato are at Beth Israel–Deaconess Medical Center and Harvard Medical School, 330 Brookline Avenue, Boston, MA 02215, USA.

*These authors contributed equally to this article.
†Present address: Molecular Medicine, St. James University Hospital, Leeds LS9 7TS, UK.
‡To whom correspondence should be addressed. E-mail: gdy@regpha.com

identical in amino acid sequence and ~60% identical to their Ang1 homologs. Like Ang1 (9), Ang2 has an NH_2-terminal coiled-coil domain and a COOH-terminal fibrinogen-like domain. Eight of the nine cysteines in mature Ang1 are conserved in mature Ang2; one cysteine between the coiled-coil and fibrinogen-like domains in Ang1 is absent from Ang2 (*15*).

Binding of Ang2 to Tie2 but not Tie1. We first investigated whether Ang2 was a ligand for Tie2 or for the closely related Tie1 receptor (*16*), for which a ligand has not yet been identified. We produced the ectodomains of these receptors as recombinant fusion proteins with the Fc portion of human immunoglobulin G1, coupled these Tie-Fc fusion proteins to BIAcore sensor chips (Pharmacia), and then measured the binding of purified recombinant Ang1* [a modified form of Ang1; (*15*)] and Ang2 to these surfaces (9). Like Ang1*, Ang2 bound to the Tie2-Fc surface but not to that of Tie1-Fc (Fig. 2A). The binding of either Ang1* or Ang2 to the immobilized Tie2 ectodomains could be competitively inhibited by excess soluble Tie2-Fc but not by soluble Tie1-Fc or an irrelevant receptor-Fc fusion (Fig. 2A). When various concentrations of Tie2-Fc were assayed for binding to immobilized ligands (9) (Fig. 2B), Ang2 and Ang1 exhibited similar binding affinity for Tie2 (K_D ~3 nM, by Scatchard analysis).

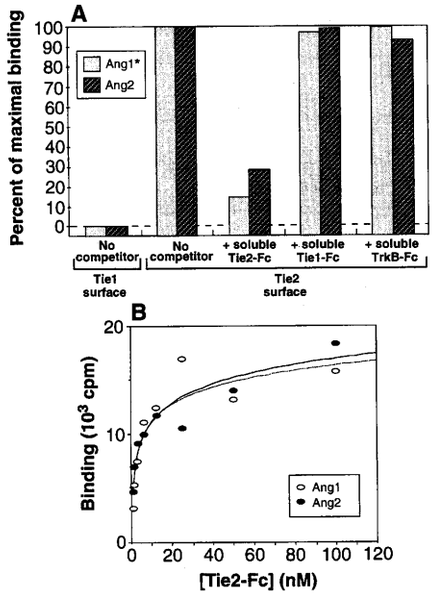

Fig. 2. Binding of Ang1 and Ang2 to the Tie receptors. (**A**) Ang1* (*15*) and Ang2 were assayed for binding to Tie1 and Tie2 receptor ectodomains coupled to BIAcore sensor chip surfaces (9) in the presence or absence of competing soluble Tie1-Fc, Tie2-Fc, or TrkB-Fc (25 μg/ml). Maximal binding of Ang1 and Ang2 to Tie2 in the absence of competitor was set to 100%, and binding to Tie1, which was negligible, was set to zero. The bars were extended below baseline for illustrative purposes. (**B**) Nitrocellulose-immobilized Ang1 and Ang2 were assayed for binding to Tie2-Fc as in (9).

Ang2 as an antagonist of Tie2. Ang1 induces rapid activation (autophosphorylation) of Tie2 receptors in endothelial cells (9). To determine whether Ang2 had this activity, we exposed a human endothelial-derived cell hybrid and a bovine endothelial cell line to conditioned media from Ang1- or Ang2-expressing cells. Ang1 caused Tie2 phosphorylation in both cell lines, whereas neither human nor mouse Ang2 had this activity (Fig. 3A). We also tested Ang2 and Ang1 on low–passage number primary cultures of human endothelial cells (Fig. 3B). Only Ang1 induced Tie2 phosphorylation. Similar results were observed even when endothelial cells were treated for varying times with a range of Ang2 concentrations (35 to 1250 ng/ml) (*17*).

Given that Ang2 binds but does not activate Tie2, we examined whether Ang2 might block Ang1 activation of Tie2. Exposure of endothelial cells to mixtures of Ang1 plus increasing concentrations of Ang2 showed that a fourfold to eightfold molar excess of Ang2 substantially blocks Ang1 activity (Fig. 3C). This result suggests that the natural role of Ang2 may be to antagonize Ang1 activation of Tie2.

In NIH 3T3 fibroblasts, Ang2 was equivalent to Ang1 in inducing the phosphorylation of ectopically expressed Tie2 receptors (Fig. 3D), an indication that Ang2 acts as an antagonist for Tie2 in the context of an endothelial cell but not in other cell types. Hence, endothelial cells may contain unique components that interact with Tie2 and allow functional discrimination between the two angiopoietins.

Ang1 and Ang2 expression in the mouse embryo. In mid-gestational mouse embryos, Ang1 transcripts were abundant in the myocardium of both atrium and ventricle (Fig. 4, A and C) (*13*) and in mesenchymal and smooth muscle cells surrounding most blood vessels, including the dorsal aorta and vessels of neural tissues, the somites, and lung (Fig. 4A). Ang1 transcripts were also prominent in clusters of three to four cells within the fetal liver parenchyma (Fig. 4E). These cells do not appear to be endothelial cells, smooth muscle cells, or associated pericytes, but may be sites of hemopoiesis.

In contrast, Ang2 transcripts were not readily detected in the developing heart but were abundant in the dorsal aorta and major aortic branches (Fig. 4, B and D), specifically in the smooth muscle layer beneath the vessel endothelium (Fig. 4D). Both Ang2 and Ang1 were associated with the embryonic vasculature, although Ang2 had a more punctate pattern. For example, Ang2 transcripts in fetal liver were localized to cells at or close to the lumen of hepatic vessels and were not present over all vessels in a given section (Fig. 4F). These Ang2-positive cells are likely to be endothelial cells or closely associated pericytes (*18*). The distinct but overlapping expression pattern of Ang1 and Ang2 is consistent with the possibility that Ang2 may regulate Ang1 function at particular sites and stages of vascular development.

Expression of Ang2 in adult tissues that undergo vascular remodeling. To explore angiopoietin expression in the adult,

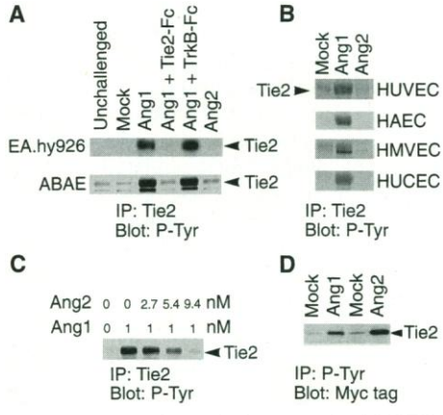

Fig. 3. Effects of Ang1 and Ang2 on Tie2 receptor phosphorylation. (**A**) A human endothelial cell hybrid [EA.hy926, an immortalized hybrid of human umbilical vein endothelial cells (HUVEC) and the A-549 human lung carcinoma line (*26*)] and an adult bovine aortic endothelial (ABAE) line were serum-starved and incubated with conditioned media from COS cells transfected with empty vector (mock) or vectors encoding human Ang1 or human Ang2. Tie2 receptor tyrosine phosphorylation was then visualized by immunoblot analysis (9). Ang1 stimulation of Tie2 was blocked by addition to the medium of excess soluble Tie2-Fc, but not TrkB-Fc. (**B**) Lack of Ang2 activation of Tie2 in human endothelial cells. Four types of low–passage number human endothelial cells [HUVEC, human aortic (HAEC), human dermal microvascular (HMVEC; Clonetics, San Diego), and human cutaneous fat pad microvascular (HUCEC) endothelial cells] were treated and assayed as in (A). (**C**) Inhibition of Ang1 activation of Tie2 by Ang2. EA.hy926 cells were serum-starved, treated with mixtures containing Ang1 and increasing concentrations of Ang2, and assayed as above. (**D**) Activation by Ang2 of Tie2 receptors ectopically expressed in nonendothelial cells. NIH 3T3 fibroblasts stably expressing transfected Tie2 receptors were treated with conditioned media and assayed as above. The transfected receptors were genetically engineered to decrease basal amounts of receptor phosphorylation (*27*) and contained a COOH-terminal c-Myc epitope tag.

we first performed Northern blot analyses of RNA from adult human tissues (Fig. 5). Ang1 was widely expressed, although in small amounts in the heart and liver. By contrast, Ang2 expression was readily detectable only in ovary, placenta, and uterus, which are the three predominant sites of vascular remodeling in the normal adult.

We next analyzed angiopoietin expression in the rat ovary, where vascular remodeling and VEGF expression have been well characterized (*19*). Ovarian follicle development depends on sequential regulation of vascular outgrowth and vascular regression. At maturation, the follicle ruptures, expels the ovum, and then undergoes reorganization into a cell-dense secretory structure known as the corpus luteum. This process includes a wave of vascular sprouting and ingrowth that hypervascularizes the corpus luteum; these vessels eventually regress as the corpus luteum ages. In agreement with previous observations (*19*), we found that VEGF mRNA was present in the preovulatory follicle before vessel invasion, first detectable in cells of the stratum granulosum that surround the ovum, and later throughout the inner part of the granulosum layer (Fig. 6C, columns 1 and 2). In the initial phase of vessel invasion, VEGF mRNA was abundant within the center of the developing corpus luteum, including regions where vessels had not yet formed (Fig. 6C, column 3). In contrast, Ang1 transcripts were associated with blood vessels and appeared to follow or coincide with, rather than precede, vessel ingrowth into the early corpus luteum (Fig. 6E, columns 1 to 3). These observations are consistent with the hypothesis (*9*, *13*) that Ang1 has a later role than VEGF in angiogenesis, perhaps involving vessel maturation or stabilization (or both). The pattern of Ang2 expression, however, suggests that this factor plays an early role at the sites of vessel invasion. Initially, Ang2 transcripts were clustered in close association with blood vessels in the theca interna of the late preovulatory follicle (Fig. 6D, column 2 versus column 1), and then were abundant at the front of vessels invading the developing corpus luteum (Fig. 6D, column 3). These expression patterns suggest that Ang2 may collaborate with VEGF at the front of invading vascular sprouts by blocking a constitutive stabilizing or maturing function of Ang1, and thus allowing vessels to revert to, and remain in, a more plastic state where they may be more responsive to a sprouting signal provided by VEGF.

In follicular atresia, a condition in which large vesicular follicles fail to ovulate, there is no invasion of vessels into the stratum granulosum, and the surrounding vessels in the theca interna recede as the follicle regresses. VEGF mRNA was not detectable in atretic follicles (Fig. 6C, column 4), whereas Ang2 mRNA was present in uniformly large amounts within the granulosum (Fig. 6D, column 4). Aged corpora lutei, in which vessels degenerate, also showed small amounts of VEGF mRNA but large amounts of Ang2 mRNA (*17*). One interpretation of these expression patterns is that in the presence of abundant VEGF, Ang2 can promote vessel sprouting by blocking a constitutive (stabilizing) Ang1 signal, whereas in the absence of VEGF,

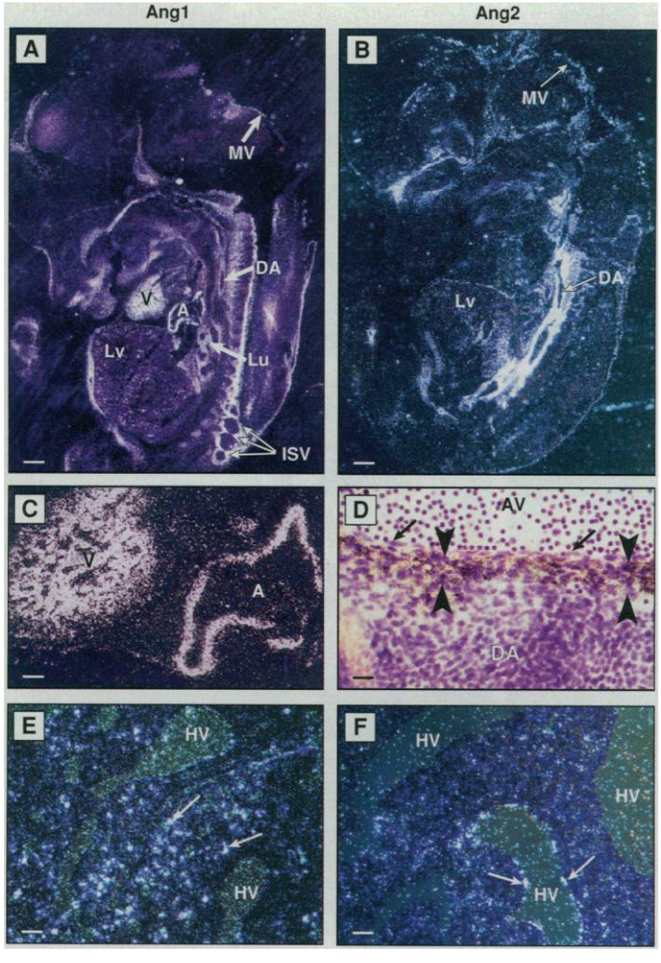

Fig. 4. Comparison of Ang1 and Ang2 mRNA expression patterns in E12.5 mouse embryos. (**A** and **B**) Dark-field views of sagittally sectioned embryos. Abbreviations: DA, dorsal aorta; Lv, liver; V, ventricle; A, atrium; MV, meningeal vessels; Lu, lung; and ISV, intersegmental vessels. Scale bars, 200 μm. (**C**) Dark-field view showing Ang1 mRNA expression in the myocardium of ventricle (V) and atrium (A). Scale bar, 50 μm. (**D**) Bright-field view showing Ang2 mRNA expression (black grains) in smooth muscle layer of dorsal aorta but not in endothelial cells. Black arrowheads delimit smooth muscle layer; arrows indicate endothelial cells. AV, aortic vessel. Scale bar, 25 μm. (**E**) Dark-field view of fetal liver showing punctate pattern of Ang1 mRNA expression in clusters of three to four cells (arrows) within the parenchyma. HV, hepatic vessel. Scale bar, 100 μm. (**F**) Dark-field view of fetal liver showing punctate pattern of Ang2 mRNA expression. The hybridization signals (arrows) were associated with endothelial-like cells at the vessel lumen, and were present only on a subset of hepatic vessels (HV). Scale bar, 100 μm. In situ hybridizations were performed as in (*13*) with probes as described (*28*).

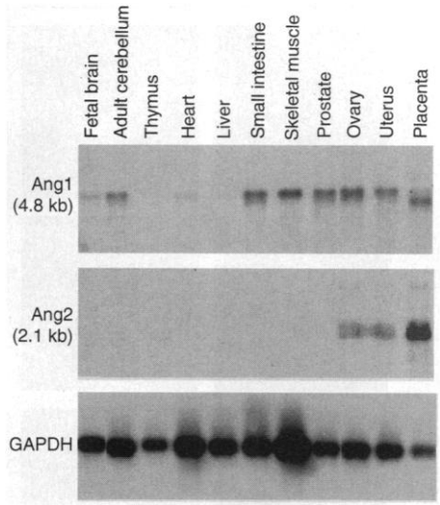

Fig. 5. Expression of Ang2 mRNAs in adult human tissues. Polyadenylated [poly(A)$^+$] RNAs (2 μg) from the indicated human fetal brain and adult tissues (Clontech) were fractionated on duplicate agarose gels, transferred to nylon membranes, and hybridized with radiolabeled cDNA as in (*25*). Probes spanned the coding regions of human Ang1 and Ang2 cDNAs. One filter was rehybridized with a glyceraldehyde-3-phosphate dehydrogenase (GAPDH) cDNA probe to control for RNA sample loading. The lower Ang1 band (~4.6 versus 4.8 kb) seen in placenta reflected variation in Ang1 transcript poly(A)-site preference. A similar expression profile was seen with mouse and rat RNAs.

Ang2 inhibition of a constitutive Ang1 signal can contribute to vessel regression. Thus, angiopoietin titration of the activation state of the Tie2 receptor may regulate the plasticity of endothelial cells and thereby modify their requirement for, and responsiveness to, VEGF.

Disruption of vessel formation in vivo by transgenic overexpression of Ang2. To test the hypothesis that Ang2 negatively regulates Tie2 function in vivo, we generated transgenic mice specifically overexpressing Ang2 in their blood vessels. This was accomplished with the use of an expression vector containing Tie2 transcriptional regulatory elements, which direct expression of introduced genes to virtually all vascular structures in a developing mouse embryo (*20*). Because endogenous Ang2, unlike Ang1, is not expressed either in developing heart or around any other vascular beds at early embryonic stages [embryonic day (E) 9–10.5] (*17*), vascular overexpression of a Tie2 antagonist might be expected to mimic some of the defects observed at these ages in mouse embryos lacking Ang1 or its receptor (*12, 13*). Pilot injections of the Ang2 expression construct produced no transgenic newborn pups (*17*). A total of six independently derived transgenic embryos were analyzed at E9–9.5, the only developmental age examined in detail (transgenic embryos died at E9.5–10.5). In situ hybridization analysis verified transgenic Ang2 expression in vascular endothelium (*17*).

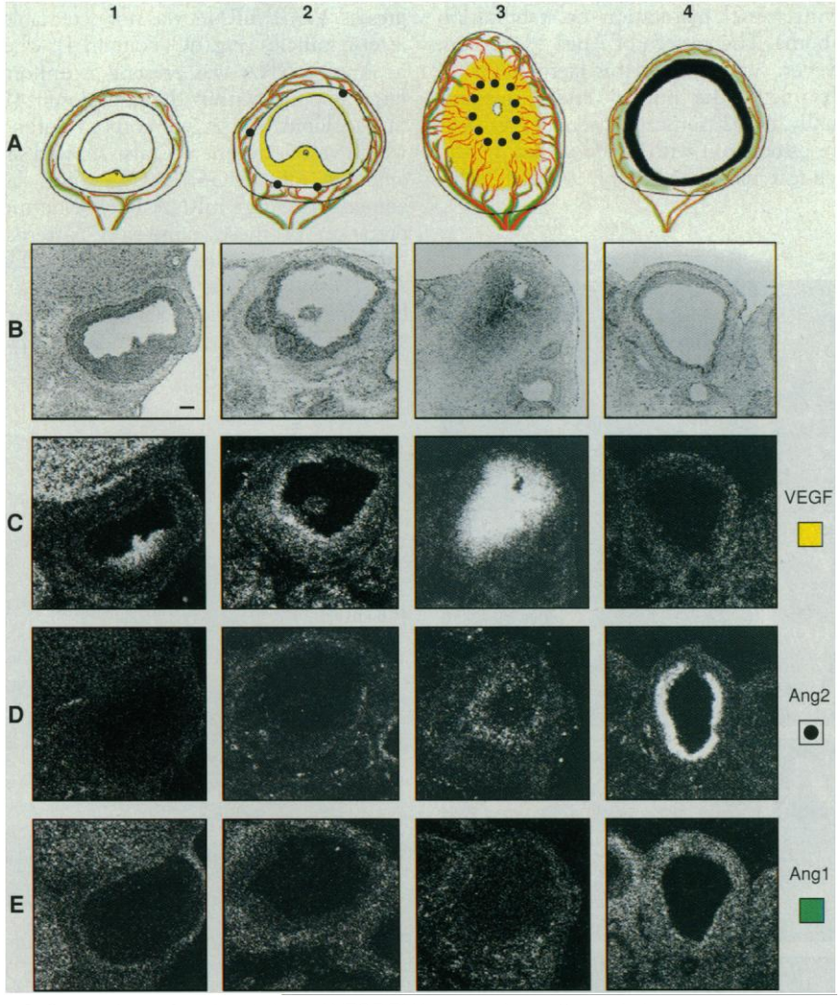

Fig. 6. Comparison of angiopoietin and VEGF RNA expression patterns during vascular remodeling in the ovary. Ovaries from hormone-induced ovulating rats (*29*) were serially sectioned and adjacent 8-μm sections were hybridized to the indicated probes. Sections correspond to three successive developmental stages: a small vesicular follicle (column 1), a large preovulatory follicle (column 2), and a developing corpus luteum ~8 hours after ovulation (column 3). Also shown is a nonproductive follicle undergoing atretic regression (column 4). (**A**) Schematic summary of the RNA expression patterns relative to the known disposition of the vasculature (red) during the various stages of follicular development and atresia. VEGF, yellow; Ang1, green; Ang2, large black dots in late preovulatory follicle and corpus luteum (columns 2 and 3) and solid black region in atretic follicle (column 4). (**B**) Corresponding bright-field images of each developmental stage. (**C** to **E**) Dark-field images of sections probed for transcripts of VEGF (C), Ang2 (D), or Ang1 (E). In situ hybridizations were performed as in (*13*), using probes as described (*28*). Scale bar, 100 μm (all micrographs).

All of the transgenic embryos were markedly smaller than their control littermates and exhibited the same abnormal vascular phenotype. Whole-mount platelet endothelial cell adhesion molecule–1 (PECAM) immunostaining (*13*), which highlights endothelial cells, revealed a vascular network that was "moth-eaten" in appearance because of widespread vessel discontinuities and loss of normal dendritic patterns (Fig. 7A; note the disruption of the cardinal vein in particular). Although similar to the vascular abnormalities seen in mice lacking Ang1 or Tie2 (*12, 13*), these defects in the Ang2-transgenic embryos appeared more severe. In contrast, the apparent collapse of the endocardial lining of the heart in the whole-mount stained Ang2 transgenics (Fig. 7A) was highly reminiscent of a defect seen in embryos lacking Ang1 or Tie2 (*12, 13*).

Sectioning of the Ang2 transgenics confirmed that their heart abnormalities precisely mimicked those previously observed in embryos lacking Ang1 or Tie2, with the endocardial layer detached from the myocardial surface in both ventricles and atria (Fig. 7, B to D). Moreover, the endocardial cells were not typically elongated but were rounded and not contiguous (Fig. 7, C and D). As was also seen in embryos lacking Ang1 or Tie2, the ventricular myocardium of the Ang2 transgenics did not form trabecular folds (Fig. 7D), a defect previously attributed to a failure of the abnormal endocardium to provide appropriate inductive interactions for the underlying myocardium (*12, 13*). Although most obvious in the heart, detachment of the endothelium from the underlying mesenchyme and the rounded appearance of individual endothelial cells were also observed in other vessels of the Ang2 transgenics (*17*), as in embryos lacking Ang1 or Tie2. Analysis of sections also made apparent the vessel discontinuities noted in whole-mount transgenic embryos, and revealed that characteristic vessels were frequently absent (for example, the missing cardinal vein in Fig. 7, B and E). Endothelial cells in the vicinity of absent vessels were present in abnormal, small clusters (Fig. 7E, arrowheads).

Although the vascular defects in the Ang2-transgenic mice largely mirrored those in mice homozygous for *Ang1* or *Tie2* gene disruptions, some aspects of these defects—particularly the notable vessel discontinuities—seemed more severe. This could reflect differences in the extent and timing of the block in Tie2 signaling; that is, the *Ang2* transgene may have caused a

profound but incomplete block of Tie2 activity in the endothelial cells. Progression of vascular development in the face of variable Tie2 inhibition may have ultimately resulted in a more severe vascular phenotype. Alternatively, the more severe phenotype caused by Ang2 overexpression could reflect an activity of Ang2 that is distinct from its ability to block Ang1 activation of Tie2. For example, in some circumstances Ang2 may act as an agonist for Tie2 on particular subsets of endothelial cells, as it does on non-endothelial cells.

Conclusions. Together, the biochemical data, the angiopoietin expression patterns, and the analysis of Ang2-transgenic mice support the notion that Ang2 is a naturally occurring antagonist of Ang1 and the Tie2 receptor. The existence of related growth factor–like proteins with directly opposing actions toward a receptor tyrosine kinase has previously been noted only in *Drosophila*, where the related protein ligands Argos and Spitz appear to have opposite effects on the epidermal growth factor receptor homolog Torso (*21*). The closest parallel in vertebrates is the apparent inhibition of the Met receptor tyrosine kinase by truncated forms of hepatocyte growth factor (*22*). Among cytokines and their receptors, interleukin-1 (IL-1) and the IL-1 receptor antagonist (IL1Ra) have opposing actions on their receptor (*23*). Ang2 may be one of many receptor tyrosine kinase antagonists to be discovered in vertebrates. Alternatively, the Tie2 receptor may be unusual in requiring regulation by both positive and negative factors; the need for such precise regulation is consistent with the proposal that point mutations affecting Tie2 activity cause vascular malformations in humans (*24*).

The evidence to date indicates that the angiopoietins and Tie2 do not participate in the initial vasculogenic phase of vascular development, but rather play critical roles in angiogenic outgrowth, vessel remodeling, and maturation (*12*, *13*). In these later developmental phases, the angiopoietins and Tie2 appear to be required for communication of endothelial cells with the surrounding mesenchyme in order to establish stable cellular and biochemical interactions. On the basis of our data, positive or negative regulation of Tie2 is likely to result in different outcomes depending on the combination of simultaneously acting angiogenic signals. For example, although Ang1 may provide a maturation or stabilization signal through Tie2 that can be blocked by Ang2, such inhibition may result in continued remodeling or the initiation of vascular sprouting in the context of simultaneous VEGF exposure but may result in frank vessel regression in the absence of VEGF. Therapeutic manipulation of vessel growth—either positively to promote revascularization or negatively to prevent tumor growth—is likely to require simultaneous regulation of both the VEGF and angiopoietin systems. Ang1 and Ang2 provide for naturally occurring positive and negative regulators of angiogenesis that can now be further tested for their ability to manipulate vessel formation, alone and in combination with other agents, in therapeutically beneficial ways.

Our findings show that Ang2 acts as an

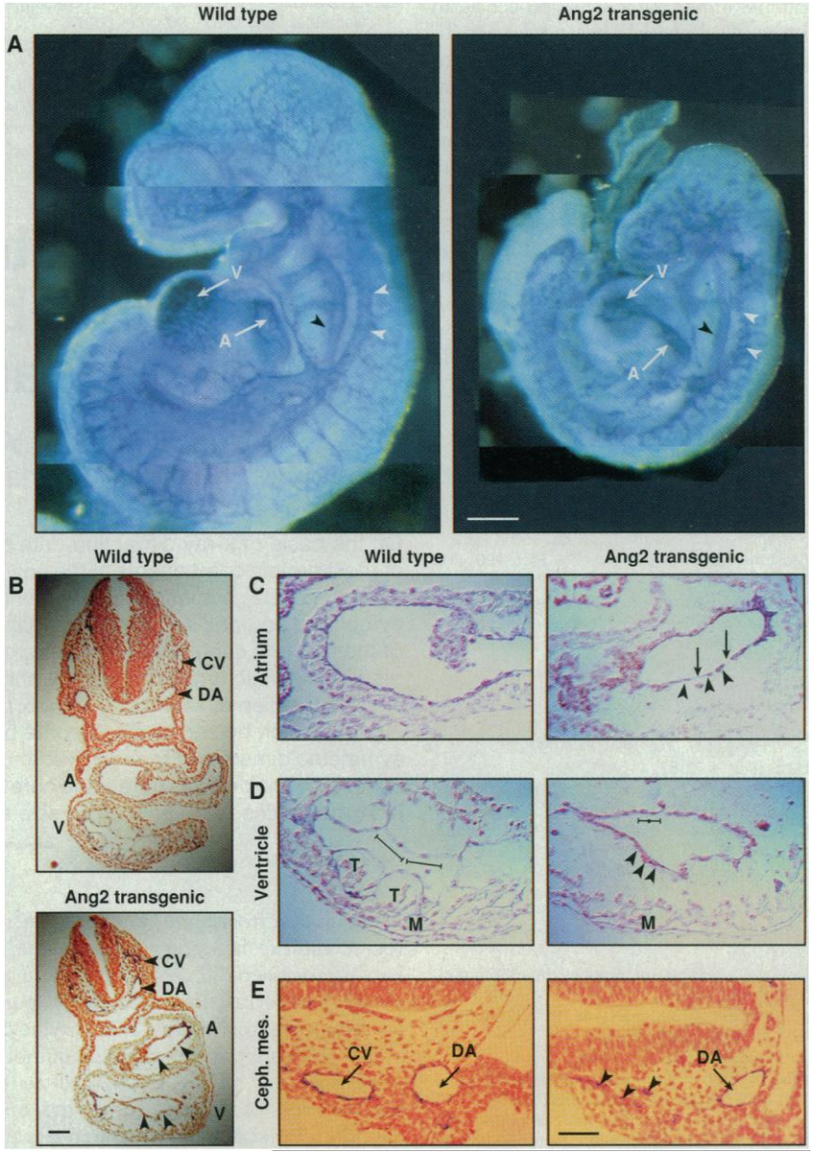

Fig. 7. Phenotype of embryos overexpressing Ang2. (**A**) Whole-mount PECAM-stained Ang2 transgenic and wild-type embryos at ~E9–9.5. The Ang2 transgenic is smaller. It has collapsed heart endocardium, various vascular abnormalities in and around the heart, and lacked a regular dendritic capillary plexus in the head, reminiscent of defects in embryos lacking Ang1 or Tie2 (*12*, *13*). Many discontinuous vessels, including the cardinal vein (white arrowheads), can be seen, although the anterior portion of the dorsal aorta is relatively unaffected (black arrowhead). Scale bar, 300 μm. (**B** to **E**) Sectioned whole-mount PECAM-stained embryos. In (B), in the atrium and ventricle of the Ang2 transgenic, arrowheads point to collapsed endocardium separated from underlying myocardium. Note missing cardinal vein but intact dorsal aorta in the Ang2 transgenic. In (C) and (D), a high-magnification view of atria and ventricles shows that in the Ang2 transgenic, endocardium (arrowheads) is separated from the underlying myocardium, endocardial cells are abnormally shortened and rounded (lines demarcate two adjacent endothelial cells), and there are interruptions in the endocardial layer (arrows) with an absence of trabeculae lined with endocardial folds. In (E), sectioned cephalic mesenchyme shows endothelial cells in abnormal, small clusters (arrowheads) at the site of the missing cardinal vein. Abbreviations: A, atrium; V, ventricle; CV, cardinal vein; DA, dorsal aorta; M, myocardium; and T, trabeculae. Scale bars, 100 μm.

antagonist for Tie2 receptors expressed on endothelial cells in vitro and in vivo. However, we also unexpectedly found that Ang2 acts as an agonist for Tie2 receptors ectopically expressed on nonendothelial cells (fibroblasts). One possible explanation for these disparate effects is that endothelial cells express an accessory component or components required for Ang2 to act as an antagonist. Tie1, which has no known ligand and is expressed predominantly in endothelial cells, may be such a component, perhaps by undergoing Ang2-induced heterodimerization with Tie2 and thus preventing Tie2 activation; however, preliminary evidence argues against this possibility (*17*). The observation that Ang2 can activate Tie2 on certain cultured cells raises the question of whether this activation occurs in vivo, perhaps in a special subclass of endothelial cells, or in the rare nonendothelial cell types that express Tie2, such as the early cells of the hemopoietic lineage (*11*).

REFERENCES AND NOTES

1. W. Risau, *FASEB J.* **9**, 926 (1995); *Nature* **386**, 671 (1997).
2. J. Folkman, *Nature Med.* **1**, 27 (1995).
3. D. Hanahan and J. Folkman, *Cell* **86**, 353 (1996).
4. T. Mustonen and K. Alitalo, *J. Cell Biol.* **129**, 895 (1995).
5. G. H. Fong, J. Rossant, M. Gertenstein, M. L. Breitman, *Nature* **376**, 66 (1995); F. Shalaby *et al.*, *ibid.*, p. 62; P. Carmeliet *et al.*, *ibid.* **380**, 435 (1996); N. Ferrara *et al.*, *ibid.*, p. 439.
6. D. Jackson, O. V. Volpert, N. Bouck, D. I. H. Linzer, *Science* **266**, 1581 (1994).
7. M. S. O'Reilly *et al.*, *Cell* **79**, 315 (1994).
8. M. S. O'Reilly *et al.*, *ibid.* **88**, 277 (1997).
9. S. Davis *et al.*, *ibid.* **87**, 1161 (1996).
10. D. J. Dumont, T. P. Yamaguchi, R. A. Conlon, J. Rossant, M. L. Breitman, *Oncogene* **7**, 1471 (1992); P. C. Maisonpierre, M. Goldfarb, G. D. Yancopoulos, G. Gao, *ibid.* **8**, 1631 (1993); T. N. Sato, Y. Qin, C. A. Kozak, K. L. Audus, *Proc. Natl. Acad. Sci. U.S.A.* **90**, 9355 (1993); H. Schnurch and W. Risau, *Development* **119**, 957 (1993); S. F. Ziegler, T. A. Bird, K. A. Schneringer, K. A. Schooley, P. R. Baum, *Oncogene* **8**, 663 (1993).
11. A. Iwama *et al.*, *Biochem. Biophys. Res. Commun.* **195**, 301 (1993).
12. D. J. Dumont *et al.*, *Genes Dev.* **8**, 1897 (1994); T. N. Sato *et al.*, *Nature* **376**, 70 (1995).
13. C. Suri *et al.*, *Cell* **87**, 1171 (1996).
14. Cloning of Ang2 cDNAs resulted from screening a human fetal lung and a mouse adult uterus cDNA library (both from Clontech) with the full-length mouse ^{32}P-labeled Ang1 cDNA probe at 55° or 65°C (*25*).
15. Mutation of Cys^{245} in Ang1, which is not shared between Ang1 and Ang2, does not alter its agonistic properties. For some experiments, Ang1* (a recombinant version of Ang1 with a modified NH_2-terminus and mutated Cys^{245} that is easier to produce and purify) was used instead of Ang1; for details on expression and purification of Ang1, Ang1*, and Ang2, see S. Davis *et al.*, in preparation.
16. J. Partanen *et al.*, *Mol. Cell. Biol.* **12**, 1698 (1992).
17. P. C. Maisonpierre *et al.*, data not shown.
18. K. K. Hirschi and P. A. D'Amore, *Cardiovasc. Res.* **32**, 687 (1996).
19. J. K. Findlay, *J. Endocrinol.* **111**, 357 (1986); H. S. Phillips, J. Hains, D. W. Leung, N. Ferrara, *Endocrinology* **127**, 965 (1990); D. Shweiki, A. Itin, G. Neufeld, H. Gitay-Goren, E. Keshet, *J. Clin. Invest.* **91**, 2235 (1993); E. Bacharach, A. Itin, E. Keshet, *Proc. Natl. Acad. Sci. U.S.A.* **89**, 10686 (1992).
20. T. M. Schlaeger *et al.*, *Proc. Natl. Acad. Sci. U.S.A.* **94**, 3058 (1997).
21. R. Schweitzer, R. Howes, R. Smith, B.-Z. Shilo, M. Freeman, *Nature* **376**, 699 (1995).
22. V. Cioce *et al.*, *J. Biol. Chem.* **271**, 13110 (1996).
23. W. P. Arend, H. G. Welgus, R. C. Thompson, S. P. Eisenberg, *J. Clin. Invest.* **85**, 1694 (1990).
24. M. Vikkula *et al.*, *Cell* **87**, 1181 (1996).
25. P. C. Maisonpierre *et al.*, *Science* **247**, 1446 (1990).
26. C.-J. S. Edgell, C. C. McDonald, J. B. Graham, *Proc. Natl. Acad. Sci. U.S.A.* **80**, 3734 (1983).
27. P. C. Maisonpierre, P. F. Jones, S. Davis, G. D. Yancopoulos, in preparation.
28. Probes for mouse embryo sections were 560- and 680-nucleotide (nt) cRNAs extending from 5′ leader sequence to, respectively, codon 165 in mouse Ang1 cDNA and codon 155 in mouse Ang2 cDNA. Probes for rat ovary sections were VEGF, a 141-nt cRNA spanning the last 47 rat VEGF codons (which are shared among most VEGF RNA splice-variants); Ang1, a 773-nt cRNA spanning the last 257 codons of mouse Ang1 cDNA; and Ang2, a 315-nt cRNA spanning codons 380 to 485 in rat Ang2 cDNA.
29. To obtain staged ovulating ovarian tissue, we injected immature (postnatal day 29) female Sprague-Dawley rats (Zivic-Miller) with 5 U of pregnant mare serum gonadotropin (Calbiochem). Rats were killed and ovaries were surgically removed beginning at 56 hours after injection and at 9- to 32-hour intervals thereafter.

30. We thank L. S. Schleifer and P. R. Vagelos for enthusiastic support; M. Goldfarb, M. Wang, R. Rossman, D. Datta, Y. Qing, T. Schlaeger, J. Lawitts, and J. Bruno for their contributions; J. Springhorn for HUCEC cells; and C. Murphy, E. Hubel, C. Rudowsky, and E. Burrows for graphics work. T.N.S. was partly supported by Hoffmann–LaRoche Inc.

7 March 1997; accepted 13 May 1997

Crystal Structure of the Cytochrome bc_1 Complex from Bovine Heart Mitochondria

Di Xia, Chang-An Yu, Hoeon Kim, Jia-Zhi Xia, Anatoly M. Kachurin, Li Zhang, Linda Yu, Johann Deisenhofer*

On the basis of x-ray diffraction data to a resolution of 2.9 angstroms, atomic models of most protein components of the bovine cytochrome bc_1 complex were built, including core 1, core 2, cytochrome b, subunit 6, subunit 7, a carboxyl-terminal fragment of cytochrome c_1, and an amino-terminal fragment of the iron-sulfur protein. The positions of the four iron centers within the bc_1 complex and the binding sites of the two specific respiratory inhibitors antimycin A and myxothiazol were identified. The membrane-spanning region of each bc_1 complex monomer consists of 13 transmembrane helices, eight of which belong to cytochrome b. Closely interacting monomers are arranged as symmetric dimers and form cavities through which the inhibitor binding pockets can be accessed. The proteins core 1 and core 2 are structurally similar to each other and consist of two domains of roughly equal size and identical folding topology.

Ubiquinol–cytochrome c oxidoreductase (bc_1 complex) is a component of the eukaryotic or bacterial respiratory chain and of the photosynthetic apparatus in purple bacteria. In mitochondria, this enzyme catalyzes electron transfer from ubiquinol to cytochrome c, which is coupled to the translocation of protons across the mitochondrial inner membrane from the matrix space (negative or N side) to the intermembrane space (positive or P side). Thus, bc_1 contributes to the electrochemical proton gradient that drives adenosine triphosphate (ATP) synthesis (*1*). The purified mitochondrial bc_1 complex contains 11 protein subunits (*2*, *3*); it consists of 2165 amino acid residues and four prosthetic groups with a total molecular mass of 248 kD. The amino acid sequences of all subunits are known; some of them were determined by peptide sequencing (*4*) and others were deduced from nucleotide sequences (*5*). The essential redox components of bc_1 are the two b-type hemes b_L (also called b_{565}) and b_H (b_{562}), one c-type heme (c_1), one high-potential iron-sulfur cluster (2Fe-2S Rieske center), and ubiquinone.

On the basis of functional data (*1*), the proton-motive Q cycle has been favored as a model for bc_1 function (*6*). The key feature of the model is that there are two separate ubiquinone or ubiquinol binding sites; ubiquinol is oxidized at site Q_o, near the P side of the inner mitochondrial membrane, and ubiquinone is reduced at site Q_i, near the N side of the membrane. According to the Q cycle model, one electron is transferred from ubiquinol to the Rieske

D. Xia, H. Kim, and J. Deisenhofer are in the Howard Hughes Medical Institute and Department of Biochemistry, University of Texas Southwestern Medical Center, Dallas, TX 75235, USA. C.-A. Yu, J.-Z. Xia, A. M. Kachurin, L. Zhang, and L. Yu are in the Department of Biochemistry and Molecular Biology, Oklahoma State University, Stillwater, OK 74078, USA.

*To whom correspondence should be addressed. E-mail: jd@howie.swmed.edu